ELSEVIER

Clinical Neurophysiology 111 (2000) 417–427

www.elsevier.com/locate/clinph

Topographical characteristics of slow wave activities during the transition from wakefulness to sleep

Hideki Tanaka[a,b,1], Mitsuo Hayashi[b], Tadao Hori[b,*]

[a]*Department of Behavioral Sciences, Faculty of Integrated Arts and Sciences, Hiroshima University, 1-7-1, Kagamiyama, Higashi-Hiroshima, 739-8521, Japan*

[b]*Geriatric Mental Health, National Institute of Mental Health, National Center of Neurology and Psychiatry, 1-7-3 Kohnodai, Ichikawa, 272-0827, Japan*

Accepted 20 September 1999

Abstract

Objectives: This study examined the topographical characteristics of slow wave(delta and theta) activities during the transition from wakefulness to sleep, using topographic mapping of EEG power and coherence.

Methods: Sonography of nocturnal sleep was recorded on 10 male subjects. Each recording, from 'lights-off' to 5 min after the appearance of the first sleep spindles, was analyzed. Typical EEG patterns during the transition from wakefulness to sleep were classified into 9 stages (EEG stages).

Results and conclusions: Topographic maps of coherence in delta-and theta-band activities demonstrated that the synchronous component at the anterior-central areas of the scalp appeared corresponding with increasing power. The populations of high coherence pairs among total pairs were computed for each band and each EEG stage to examine the regional differences of EEG. The populations of the delta-band activity increased clearly from EEG stage 6 in the anterior-central areas. The populations of the theta-band activity increased clearly from EEG stage 7 in the anterior-central areas. These results suggest that the dominant synchronous component of slow wave activities during the transition from wakefulness to sleep increased as a function of EEG stages in the anterior-central areas and increased clearly after the appearance of vertex sharp waves.

Keywords: Coherence; Sleep onset period; Slow wave activities; Topographic maps

1. Introduction

Examining the relationships between physiological changes and behavioral, subjective changes that occur during the transition from wakefulness to sleep will facilitate understanding of brain function during wakefulness and sleep. The brain undergoes meaning functional modifications that are reflected in electroencephalogram (EEG) activity and its own metabolic rate during sleep (Guevara et al., 1995). Because EEG variations during the transition from wakefulness to sleep were remarkable, early investigators (Davis et al., 1938; Gibbs and Gibbs, 1950; Shiotsuki et al., 1954) noted the characteristics of the waveforms and frequencies of EEG during the transition from wakefulness to sleep and classified them. However, using standard sleep criteria (Rechtschaffen and Kales, 1968), most EEG patterns during the transition from wakefulness to sleep have been combined into standard sleep stage 1.

Studies (Hori et al., 1990; Hasan and Broughton, 1994) that examined the topographical behavior of EEG activity in the sleep onset period (SOP) indicated that such topograms were useful for illustrating the characteristics of EEG changes that the early investigators noted on qualitative EEG studies (Davis et al., 1938; Gibbs and Gibbs, 1950; Dement and Keitman,1957; Foulkes and Vogel, 1965). When the topographical behavior of EEG in the SOP is of interest, however, the standard sleep stage criteria, especially for sleep stage 1, are too vague to define when the convergence of behavioral, subjective and polygraphical measures in the SOP is being studied.

Therefore, to examine the EEG variations of the SOP, typical EEG patterns during the waking-sleeping transition period were classified into 9 EEG stages (Hori et al., 1991, 1994; Tanaka et al., 1996). Nine EEG stages are effective for detailing the sleep stage 1 latency of the multiple sleep latency test (MSLT) or of the repeated test of sustained

* Corresponding author. Tel.: +81-824-246-580; fax: +81-824-240-759.

E-mail addresses: tdhori@ipc.hiroshima-u.ac.jp (T. Hori) tanaka@ncap-k.go.jp (H. Tanaka)

[1] Research Fellow of the Japan Society for Promotion of Science, Tokyo, Japan.

1388-2457/00/$ - see front matter
CLINPH 99090
PII: S1388-2457(99)00253-9

wakefulness (RTSW). It excels in the sleepiness measuring method which use of stage 1 latency as the main index. Murphy et al. (1999) investigated the utility of EEG stage (the Hori 9-stage sleep onset scoring systems) in intentional sleep onset, unintentional sleep onset, narcolepsy and insomnia. And they reported that EEG stage has been shown to be a useful and sensitive method for evaluating the sleep onset period. Recently, we examined the topographical characteristics of 9 EEG stages during the transition from wakefulness to sleep (Tanaka et al., 1995, 1997). However in these studies, typically only one quantitative EEG technique was used. Therefore, it would be necessary to examine coherence analyses of the EEG during the transition from wakefulness to sleep, which is a measure of the linear correlation between two EEG derivations. The neurophysiological modifications occurring during sleep are restricted not only to local changes but also to functional differentiation between different cortical sites, as revealed by coherence analyses between two EEG signals (Shaw, 1984). Coherence is thought to be a measure of the functional and structural connectivity between two brain sites (Ford et al., 1986). Recently, decreases in alpha and beta power and decreases in alpha and beta coherence between the frontal and occipital brain sites were observed during the transition from wakefulness to sleep (Wright et al., 1995). This study used EEG power, inter-hemispheric and intra-hemispheric coherence (16 pairs) to examine spatio-temporal changes of EEG activity during transition to sleep. Although these studies were informative, the coherence analyses employed a limited number of scalp electrodes. Even if the temporal sequence were thoroughly examined, the spatial variations of those EEG patterns during the transition from wakefulness to sleep were not well considered. Furthermore, delta-band activity was not examined in detail. The EEG power density in a low frequency range corresponding to slow wave band (1–7 Hz) is an indicator of a progressively declining process during sleep (Borbely et al., 1981), and it is suggested that the slow wave band activity could be used as the parameter to describe the transition process from wakefulness to sleep. The present study focused on the slow wave band (delta-theta) activities, and examined the topographic characteristics in slow wave activities during the transition from wakefulness to sleep, using topographic mapping of EEG power and EEG coherence (66 pairs) corresponding to 9 EEG stages.

2. Materials and methods

2.1. Subjects

Ten healthy male volunteers participated in the study. Their ages ranged from 20 to 25 years (mean, 22.6 years). All subjects were undergraduate or graduate human behavior students at Hiroshima University. Each subject was given a detailed description and demonstration of the procedure and apparatus involved in the study before signing the consent form. Subjects were instructed to refrain from alcohol and drugs for 24 h prior to the experimental session and not to drink any beverage containing caffeine on the day of the study. All subjects were adapted to the recording chamber prior to the study. The waking EEG record for each subject was visually examined for alpha activity (8–13 Hz EEG activity with an amplitude more than 20 μV). Subjects with less than 50% of their waking record occupied by alpha waves were classified as low alpha subjects, while those with more than 80% were classified as the high alpha subjects. For the remaining subjects, alpha times ranged from 50 to 80%, and these were classified as the intermediate alpha subjects. All of the subjects in this study were high alpha subjects, with alpha time of 90% or more.

2.2. Apparatus

All electrophysiological parameters were recorded simultaneously on an 18-channel electroencephalograph (NEC San-Ei Model 1A97) and a 14-channel FM tape recorder (TEAC SR-50). The electroencephalograph ran at a paper speed of 10 mm/s. The EEG data were recorded by an FM tape recorder at a tape speed of 12 mm/s. A Signal Processor (NEC San-Ei Model 7T18A) was used for the subsequent off-line analysis of EEG data. The sleeper's room was a 3×3 m electrically shielded, sound attenuated and air conditioned bedroom. Temperature readings taken throughout the study showed a mean of 22.5 ± 1.0°C.

2.3. Procedure

Subjects were asked to arrive at the sleep laboratory 2 h before their usual bedtime. After changing into their nightclothes, electrodes were applied. Sleep monitoring varied slightly from that described by Rechtschaffen and Kales (1968). Thus, surface electrodes were placed on 12 scalp areas (Fp1, Fp2, F7, F8, Fz, C3, C4, Pz, T5, T6, O1, and O2) indicated by the international 10/20 system referenced to ipsilateral ear lobes (EEG), two horizontal electrooculograms (EOG), each referenced to ipsilateral ear lobes for slow eye movement ($\tau = 3.2$ s), on the chin (mentalis: EMG) referenced to each other, and on the forehead for the body ground. All electrophysiological parameters were recorded using silver–silver chloride disk electrodes filled with electrode cream and attached with either surgical tape or collodion (scalp placements). Interelectrode impedance was below 5 kΩ. The EEGs were amplified using a high- cut filter setting of 60 Hz and a time constant of 0.3 s.

The subjects were instructed to fall asleep after the light was turned off. An experimenter awakened subjects 5 min after the appearance of the first sleep spindle by calling his name via intercom and entered the room. Pre-sleep and post-sleep questionnaires were used to screen for unusual events that might be expected to influence sleep parameters.

2.4. Criteria of EEG stages during the SOP

Each recording from 'light off' to 5 min after the appearance of the first sleep spindle, was analyzed. EEG stages were also manually scored for each 5-s period of the C_3 EEG record. According to the criteria of Hori et al. (1991, 1994); Tanaka et al. (1996), the 9 EEG stages during the SOP were defined as follows.

EEG stage 1. Alpha wave train: epoch composed of a train of alpha activity with a minimal amplitude of 20 μV.

EEG stage 2. Alpha wave intermittent (A): epoch composed of a train with ⩾50% alpha activity with a minimal amplitude of 20 μV.

EEG stage 3. Alpha wave intermittent (B): epoch composed of a train with <50% alpha activity with a minimal amplitude of 20 μV.

EEG stage 4. EEG flattening: epoch composed of suppressed waves <20 μV.

EEG stage 5. Ripples: epoch composed of low voltage theta wave (20 μV $< \theta <$ 50 μV) burst suppression without a vertex sharp wave.

EEG stage 6. Vertex sharp wave solitary: epoch contained one well-defined vertex sharp wave.

EEG stage 7. Vertex sharp wave train or burst: epoch contained at least two well-defined vertex sharp waves.

EEG stage 8. Vertex sharp wave and incomplete spindle: epoch contained at least one well-defined vertex sharp wave and one incomplete spindle (duration <0.5 s, amplitude <20 μV, >10 μV).

EEG stage 9. Spindles: epoch contained at least one well-defined spindle with at least 0.5 s in duration and 20 μV amplitude.

EEG stages 1 and 2 correspond to stage W in standard criteria (Rechtschaffen and Kales), EEG stages 3–8 correspond to sleep stage 1, and EEG stage 9 corresponds to sleep stage 2. Each record was scored entirely by one scorer and then rescored by a second independent scorer. A comparison was then made between the two scorings on an epoch-by-epoch basis to determine inter-scorer reliability. The reliability score exceeded 90% for each subject's record.

2.5. EEG analysis

The polygraph data were stored on magnetic tape for later off-line analysis using an NEC San-Ei 7T18A Signal Processor with an A/D converter sampled at 5-s windows of continuous EEG activity from the light off to 5 min after the onset of standard sleep stage 2. Sample 5-s EEG records were scored and classified into 9 EEG stages. EEG sample for each stage were A/D converted at a sampling rate of 4.88 ms per point, a total of 1024 samples were taken during each 5-s sweep. A high–cut filtering at 60 Hz was used. The power spectra with 0.2 Hz resolution were computed using a fast Fourier transfomation and smoothed with a Hanning window. To reduce leakage, window modifications are necessary, which may be performed in the frequency domain. A popular procedure consists in a Hanning window, i.e. smoothing the sine and cosine series by the weights 1/4,1/2,1/4 (for data defined between 0 and T when using the FFT). Hanning leads to a much faster decay of the side lobes and reduces leakage considerably. However, spectra was attenuated to 0.375 ($0.5^2 + 0.25^2 \times 2$) level with Hanning windows. To compensate for the attenuation of the signal, multiplied 1/0.375 modified the power value.

The EEG data were then accumulated in auto-power spectra, cross-power spectra, coherence, over a frequency bandwidth of 2.0–7.4 Hz, in 5-s epochs. EEG activity was then averaged across 6 5-s epochs, providing the 30-s long spectra to be examined. A frequency bandwidth of 0.6–2.0 Hz was not examined due to concern over the slow eye movement artifacts.

The average amplitudes (square root of power) of delta (2.0–3.4 Hz), theta (3.6–7.4 Hz) were computed from 12 EEG channels. The delta- and theta- band activities were chosen to examine the activities of slow-wave activity in the SOP. Topography maps of amplitudes from consecutive EEG samples of 30-s epochs for each of the two frequency bands were computed from 12 EEG electrode placements for each of the 9 EEG stages. Each topography map of power was sectional in 10 equal steps of amplitude. The amplitude is shown in 3/5 scale for delta band activity of theta band activity.

The coherence was calculated from cross-power spectra and the corresponding auto power spectra from 6 consecutive 5-s epochs. The coherence is defined as $\mathrm{Coh}^2(\omega) = |\mathrm{Sxy}(\omega)|^2/(\mathrm{Sxx}(\omega) \times \mathrm{Syy}(\omega))$. Where $\mathrm{Sxy}(\omega)$ is the cross-power spectra and $\mathrm{Sxx}(\omega)$ and $\mathrm{Syy}(\omega)$ are the respective auto-power spectra. Coherence was computed for all 66 pairwise combinations of 12 channels. The computational procedure to obtain coherence involved first computing the power spectra and then the normalized cross-spectra.

The 66 single pair coherence data for the two frequency bands and for the 9 EEG stages were computed. To examine the topographical patterning of EEG coherence, we tried to illustrate the coherence map for each frequency band and compared those among the 9 EEG stages. At first, we illustrated the coherence [Coh (ω)] data by a wire netting method. When 66 single pair coherence values among 12 areas were lined, the wire net was too complex to understand the topographic pattern of covariant and synchronous activities. A criterion for a Coh (ω) being more than 0.7 was used as the level of coherence significance (high synchronization). Therefore, we focused on the higher coherence (⩾0.7) pairs in 3 levels (0.7 ~ 0.8, 0.8 ~ 0.9, 0.9 ~ 1.0). Artifacts were screened by visual inspection and rejection decisions were made blindly with respect to subject and EEG stage. Eye blink artifact and vertical EOG appeared at the frontal pole channels (Fp1, Fp2), therefore any epoch with eye blink artifact or vertical eye movements were rejected, referenced by the derivation Fp1 and Fp2.

2.6. Statistical analysis

For statistical purposes, amplitude (square root of power) data were log transformed and coherence values were transformed Fisher's Z scores to obtain approximation to a normal distribution. For each ANOVA, the significance level was determined following the adjusted Greenhouse–Geisser (Winer et al., 1991) approach for repeated observations. For all other analyses the standard significance level of $P < 0.05$ was used. Tukey LSD post-hoc tests were used to determine significant comparisons.

3. Results

Fig. 1 shows intra-hemispheric coherence (the upper panels) and inter-hemispheric coherence (the lower panels) for delta-band among 9 EEG stages. Because no inter-hemispheric differences in EEG power were found during transition, the right hemisphere was selected to examine intra-hemispheric differences. Intra-hemispheric coherence in anterior – central area (Fp2–F8, F8–C4) increased sharply from EEG stage 6 as a function of EEG stages. For the Fp2–F8 coherence, ANOVA indicated a main effect for EEG stages ($F(4/33) = 9.67, \epsilon = 0.46$, $P < 0.01$). The F ratios and Tukey LSD posteriori tests can be found in Table 1. Tukey LSD post hoc testing revealed that the coherence values of stages 6–9 were significantly higher than those from stages 1 to 5 (all $P < 0.05$) and the coherence values of stages 4 and 5 were significantly higher than those from stages 1 to 3 (all $P < 0.05$). For the F8–C4 coherence, ANOVA indicated a main effect for EEG stages ($F(4/38) = 9.49, \epsilon = 0.52$, $P < 0.01$). Tukey LSD post hoc testing revealed that the coherence values of stages 6–9 were significantly higher than those from stages 1 to 4 (all $P < 0.05$) and the coherence values of stages 4 and 5 were significantly higher than those from stages 1 to 3 (all $P < 0.05$). Inter-hemispheric coherence (the lower panels) in anterior – central area (F7–F8, C3–C4) increased sharply from EEG stage 6. On the other hand, inter-hemispheric coherence in area (T5–T6, O1–O2) increased sharply from EEG stage 7 (see Table 1).

Fig. 2 shows intra-hemispheric coherence (the upper panels) and inter-hemispheric coherence (the lower panels) for theta-band among 9 EEG stages. Intra-hemispheric coherence in anterior – central area (Fp2–F8, F8–C4, C4–T6) increased as a function of EEG stages. Tukey LSD posteriori comparisons confirmed the above differentiation

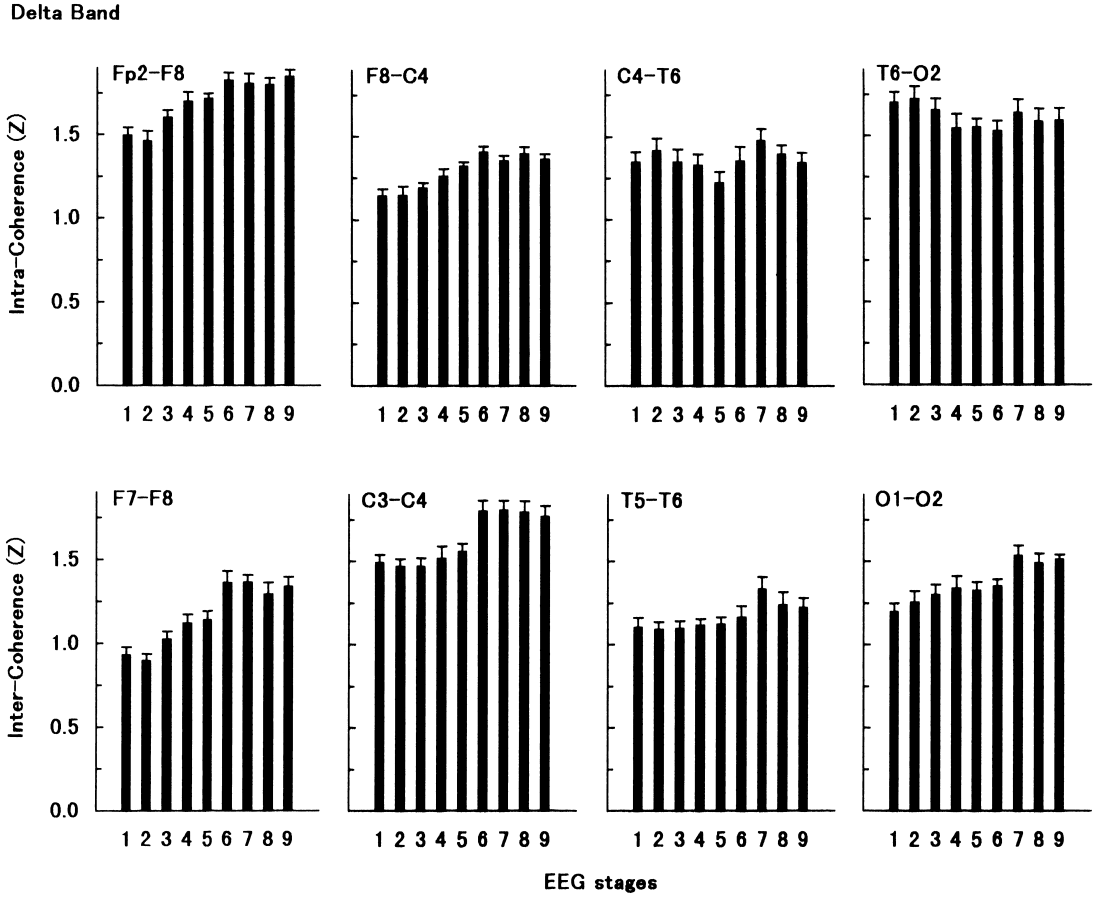

Fig. 1. Intra-hemispheric coherence (upper panels) and inter-hemispheric coherence (lower panels) for delta-band among nine EEG stages. The *X* axis shows EEG stages and the *Y* axis shows the Z-transformed coherence values. Vertical bars show the SEs.

Table 1
Mean coherence values for delta-band among 9 EEG stages. *F* ratios and Tukey LSD posteriori tests[a]

Delta band	EEG stages									*F*	d.f.	ϵ	*P*
	1	2	3	4	5	6	7	8	9				
Intra-coherence (*z*)													
Fp2–F8	1.49^{b}	1.46^{b}	1.60	1.70^{c}	1.71^{c}	1.82^{d}	1.80^{d}	1.80^{d}	1.85^{d}	9.67	4/33	0.46	<0.01
F8–C4	1.14^{b}	1.14^{b}	1.19^{b}	1.26^{c}	$1.32^{c,d}$	1.41^{e}	$1.35^{d,e}$	1.40^{e}	$1.36^{d,e}$	9.49	4/38	0.52	<0.01
Intra-coherence (*z*)													
F7–F8	0.93^{b}	0.89^{b}	1.02^{b}	1.12^{b}	1.14^{b}	1.36^{c}	1.36^{c}	1.29^{c}	1.33^{c}	18.29	4/36	0.49	<0.01
C3–C4	1.49^{b}	1.47^{b}	1.47^{b}	1.52^{b}	1.56^{b}	1.80^{c}	1.81^{c}	1.79^{c}	1.77^{c}	11.77	3/31	0.43	<0.01
T5–T6	1.10^{b}	1.09^{b}	1.10^{b}	1.12^{b}	1.12^{b}	1.17^{b}	1.33^{c}	1.24^{c}	1.22^{c}	5.68	3/25	0.34	<0.01
O1–O2	1.20^{b}	1.26^{b}	1.30^{b}	1.34^{b}	1.33^{b}	1.35^{b}	1.54^{c}	1.49^{c}	1.51^{c}	7.66	2/21	0.30	<0.01

[a] Signifcance levels are based on a Greenhouse-Geisser epsiolon adjustment. Means with the same superscript letter on the same line are not significantly different ($P > 0.05$) by Tukey LSD posteriori tests.

within each ANOVA (see Table 2). On the other hand, inter-hemispheric coherence (the lower panels) in all areas (F7–F8, C3–C4, T5–T6, O1–O2) increased sharply from EEG stage 7 (see Table 2).

To make a general survey of topographical characteristics for slow wave activities, topographic maps of power and coherence were made for delta- and theta-bands for each EEG stage. Fig. 3 shows average patterns across 10 subjects of topographical maps of power (left panel) and coherence (right panel) in delta- and theta-band activities for EEG stages (EEG stages 1–3). The numerals on the left side of this figure show the EEG stages. Thick lines show above 0.9 coherence level, thin lines show the level from 0.8 to 0.9, and broken lines show the level from 0.7 to 0.8. In these

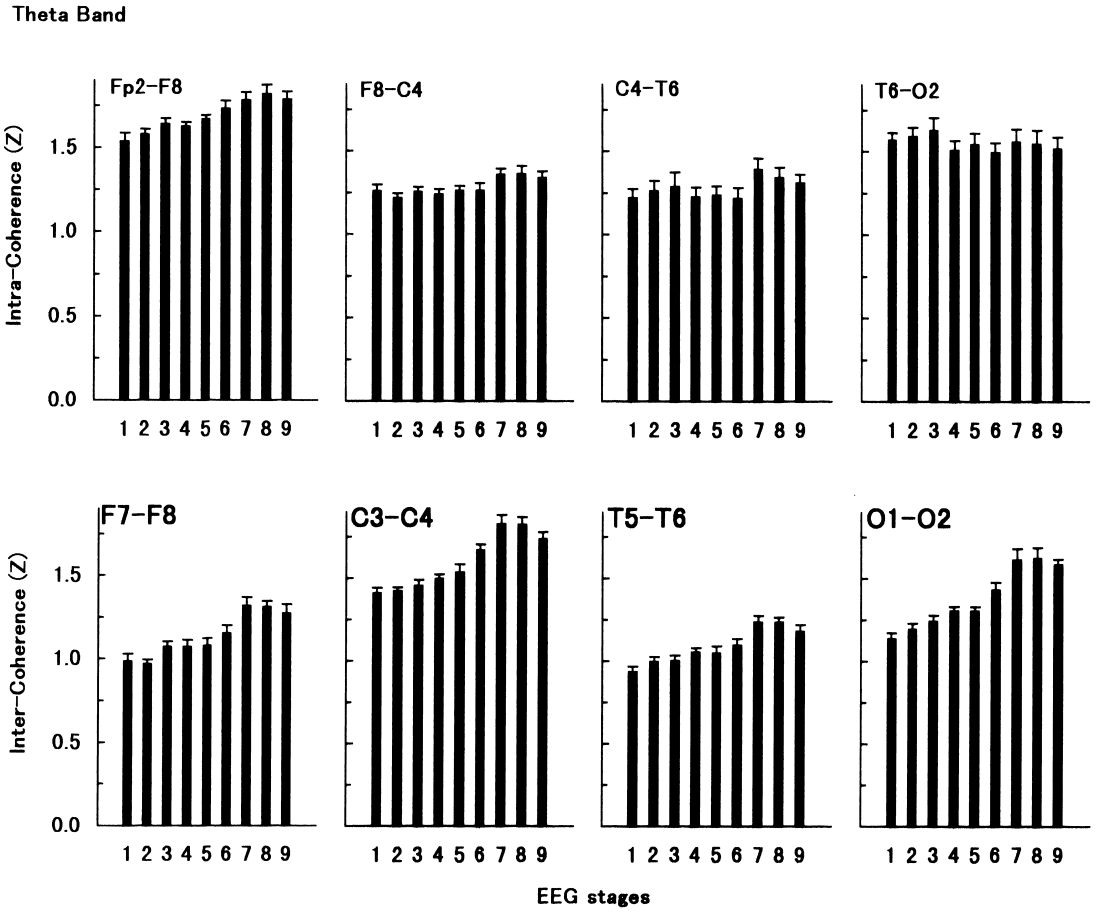

Fig. 2. Intra-hemispheric coherence (upper panels) and inter-hemispheric coherence (lower panels) for theta-band among nine EEG stages. The *X* axis shows EEG stages and the *Y* axis shows the Z-transformed coherence values. Vertical bars show the SEs.

Table 2
Mean coherence values for thet-band among nine EEG stages, F ratios and Tukey LSD posteriori tests[a]

Theta band	EEG stages									F	d.f.	ϵ	P
	1	2	3	4	5	6	7	8	9				
Intra-coherence (z)													
Fp2–F8	1.54[b]	1.58[b]	1.64[b]	1.63[b]	1.67[b]	1.73	1.78[c]	1.82[c]	1.79[c]	7.45	3/28	0.39	<0.01
F8–C4	1.26[b]	1.22[b]	1.25[b]	1.24[b]	1.26[b]	1.26[b]	1.36[c]	1.36[c]	1.34[c]	3.52	3/31	0.43	<0.05
C4–T6	1.22[b]	1.26[b]	1.29[b]	1.23[b]	1.23[b]	1.21[b]	1.39[c]	1.34[c]	1.31[c]	3.93	4/34	0.48	<0.05
Intra-coherence (z)													
F7–F8	0.98[b]	0.97[b]	1.07[b]	1.07[b]	1.08[b]	1.15[b]	1.32[c]	1.31[c]	1.27[c]	16.41	4/39	0.55	<0.01
C3–C4	1.41[b]	1.42[b]	1.46[b]	1.50[b]	1.54[b]	1.67	1.83[c]	1.83[c]	1.74[c]	27.76	4/38	0.53	<0.01
T5–T6	0.94[b]	1.00[b]	1.00[b]	1.06[b]	1.05[b]	1.10[b]	1.24[c]	1.24[c]	1.18[c]	17.82	4/38	0.52	<0.01
O1–O2	1.14[b]	1.20[b]	1.24[b]	1.31[b]	1.30[b]	1.43	1.61[c]	1.62[c]	1.58[c]	28.47	2/21	0.29	<0.01

[a] Significance levels are based on a Greenhouse–Geisser epsilon adjustment. Means with the same superscript letter on the same line are not significantly different ($P > 0.05$) by Tukey LSD posteriori tests.

stages (alpha wave stages), There were no the remarkable changes of topographic characteristics in slow wave (delta- and theta-bands) activities.

Fig. 4 shows topographical maps of power (left panel) and coherence (right panel) in delta- and theta-band activities during the period of EEG flattening (top row), ripples (second row), and vertex sharp wave solitary (bottom row). Topographic maps of power and coherence demonstrated that the power in the anterior-central areas of scalp increased as a function of EEG stages, and coherence values were also high at those areas.

Fig. 5 shows topographical maps of power (left panel) and coherence (right panel) in delta- and theta-band activities during the period of vertex sharp wave bursts (top row), vertex sharp wave and incomplete spindles (second row), and spindles (bottom row). Topographic maps of coherence in delta- and theta-band activities clearly demonstrated that the synchronous component in the anterior-central areas of scalp appeared to correspond with increasing power. Accordingly, the frequency of high coherence pairs for the 66 pairs overall were computed for each band and each EEG stage to examine the behaviors of synchronous EEG components among 9 EEG stages.

The relative frequency of high coherence pairs of 66 single pair coherence in 3 levels (from 0.7 to 0.8, from 0.8 to 0.9, above 0.9) for delta-band and for theta-band among 9 EEG stages were computed. However, there were no remarkable changes in the lower two levels (from 0.7 to 0.8, from 0.8 to 0.9) as a function of EEG stages. Fig. 6 shows that the relative frequency of high coherence pairs of 66 single pair coherence in higher levels (above 0.9) for delta-band (left) and for theta-band (right) among 9 EEG

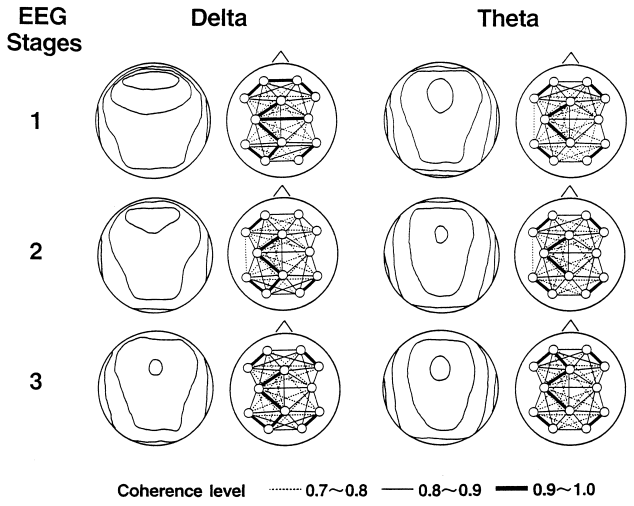

Fig. 3. Typical patterns of topographic maps of power (left panel) and coherence (right panel) for delta- and theta-frequency bands corresponding to EEG stages (EEG stages 1–3). Upper portion of each map shows the nasal and lower side shows the occipital side. The numerals on the left side of this panel indicate the 9 EEG stages. Each topographic map of power (left panel) was sliced in equal steps of amplitude.(delta, 1 step = 3.0 μV/Hz; Theta, 1 step = 1.6 μV/Hz). Thick lines of topographic maps of coherence (right panel) show above 0.9 coherence level, thin lines show the level from 0.8 to 0.9, and broken lines show the level from 0.7 to 0.8.

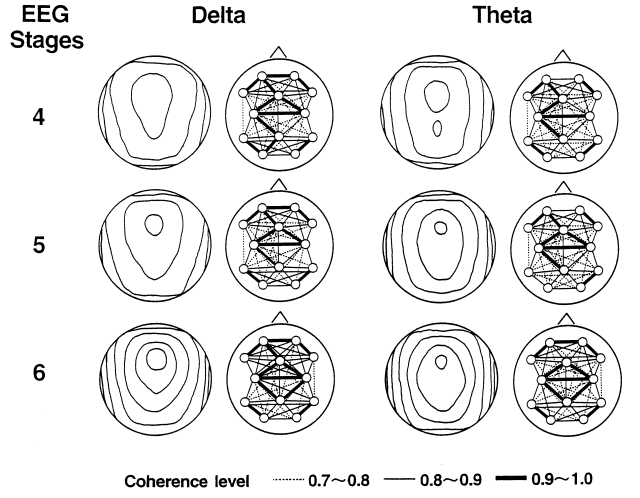

Fig. 4. Typical patterns of topographic maps of power (left panel) and coherence (right panel) for delta- and theta- frequency bands corresponding to EEG stages (EEG stages 4–6). See Fig. 3 for legend.

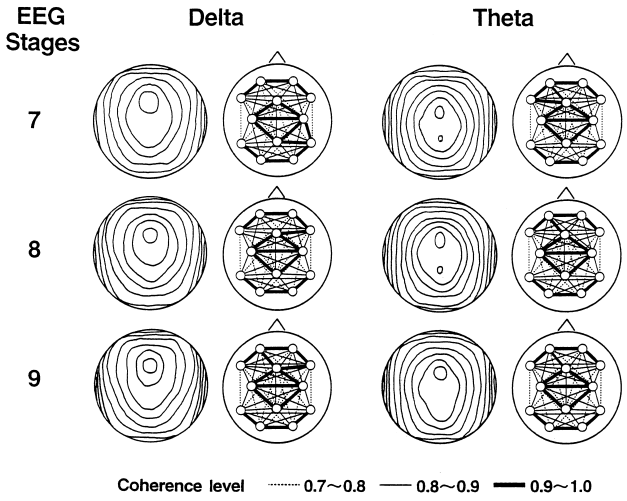

Fig. 5. Typical patterns of topographic maps of power (left panel) and coherence (right panel) for delta- and theta- frequency bands corresponding to EEG stages (EEG stages 7–9). See Fig. 3 for legend.

stages. The *X*-axis shows EEG stages and the *Y*-axis shows the population of high coherence pairs. The frequency of high coherence (above 0.9) pairs for delta-band activity clearly increased from EEG stage 6, and those for theta-band activity clearly increased from EEG stage 7. For delta-band activity, ANOVA indicated a main effect for EEG stages ($F = 8.82$, d.f. $= 4, 38$, $\epsilon = 0.53$, $P < 0.01$). Post hoc testing revealed that the population of high coherence pairs of stages 6–9 were significantly higher than those from stages1 to 5 (all $P < 0.05$). For theta-band activity, ANOVA indicated a main effect for EEG stages ($F = 15.50$, d.f. $= 4, 36$, $\epsilon = 0.50$, $P < 0.01$). Post hoc testing revealed that the population of high coherence pairs of stages 7–9 were significantly higher than those from stages 1 to 6 (all $P < 0.05$). These results indicated that delta-band activity clearly increased significantly from EEG stage 6, while theta-band activity increased significantly from EEG stage 7. Therefore, we examined the dominant region of slow wave (delta and theta) activities during the transition from wakefulness to sleep.

Fig. 7 shows the population of high coherence pairs (≥ 0.9) for total pairs for delta-band among 9 EEG stages. The left panel shows the population of high coherence pairs for the anterior area (Fp1, Fp2, F7, F8). The central panel shows the population of high coherence pairs for the central area (Fz, C3, C4, Pz). The right panel shows the population of high coherence pairs for the posterior area (T5, T6, O1, O2). The population of high coherence pairs increased from EEG stage 6 in the anterior and central areas. ANOVA (regions × EEG stages) yielded a main effect for regions ($F = 33.04$, d.f. $= 2, 15$, $\epsilon = 0.86$, $P < 0.01$) and for EEG stages ($F = 12.72$, d.f. $= 3, 29$, $\epsilon = 0.40$, $P < 0.01$) and the interaction between regions and EEG stages ($F = 3.12$, d.f. $= 5, 49$, $\epsilon = 0.34$, $P < 0.05$). Post hoc testing revealed that the population of high coherence pairs of stage 6–9 were significantly higher than those from stages 1 to 5 (all $P < 0.05$) for the anterior and central areas. However, for the posterior area, the population of high coherence pairs significantly increased momentarily only in EEG stage 7. However, significant region effects among anterior, central and posterior areas were obtained. The population of high coherence pairs (≥ 0.9) in the anterior and central areas were higher than that in the posterior area in EEG stages 5,6,8 and 9. Additionally, the population of high coherence pairs (≥ 0.9) in the central area was higher than that in the anterior area during EEG stages 6–8. These results indicate that the increased population of high coherence pairs from EEG stage 6 (as shown Fig. 6) are attributable to increased activities in the anterior and central areas, especially the central area.

Fig. 8 shows the population of high coherence pairs (≥ 0.9) for total pairs for theta-band among 9 EEG stages. The population of high coherence pairs of anterior area increased from EEG stage 7 (vertex sharp wave bursts). The population of high coherence pairs of central area increased from EEG stage 4 as a function of EEG stages, and increased sharply in EEG stage 7. There are regional differences in coherent relationships among the anterior, central and posterior areas. ANOVA yielded a main effect for regions ($F = 27.05$, d.f. $= 2, 17$, $\epsilon = 0.95$, $P < 0.01$) and for EEG stages ($F = 19.23$, d.f. $= 4, 32$, $\epsilon = 0.45$, $P < 0.01$) and the interaction between regions and EEG stages ($F = 2.33$, d.f. $= 7, 61$, $\epsilon = 0.42$, $P < 0.05$). Post hoc testing revealed that the population of high coherence pairs of stages 6–9 were significantly higher than those from stages 1 to 5 (all $P < 0.05$) for the anterior. Additionally, the population of high coherence pairs (≥ 0.9) of the central area in EEG stages 7–9 were significantly greater than those in EEG stages 1–6, and those in EEG stage 6 significantly greater than those in EEG stages 1–4. However, the population of high coherence pairs (≥ 0.9) of posterior area in EEG stage 7 was higher than those in EEG stages 4 and 5, signif-

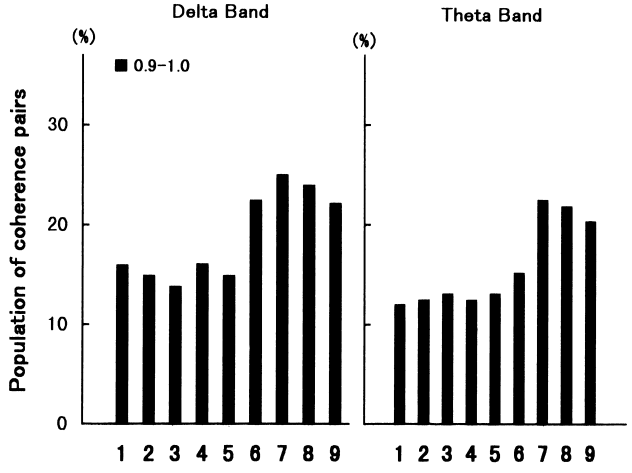

Fig. 6. Comparisons of the population of high coherence pairs (coh ≥ 0.9: root coherence) for delta-band (left) and for theta-band (right) among 9 EEG stages. The *X* axis shows EEG stages and the *Y* axis shows the population of high coherence pairs.

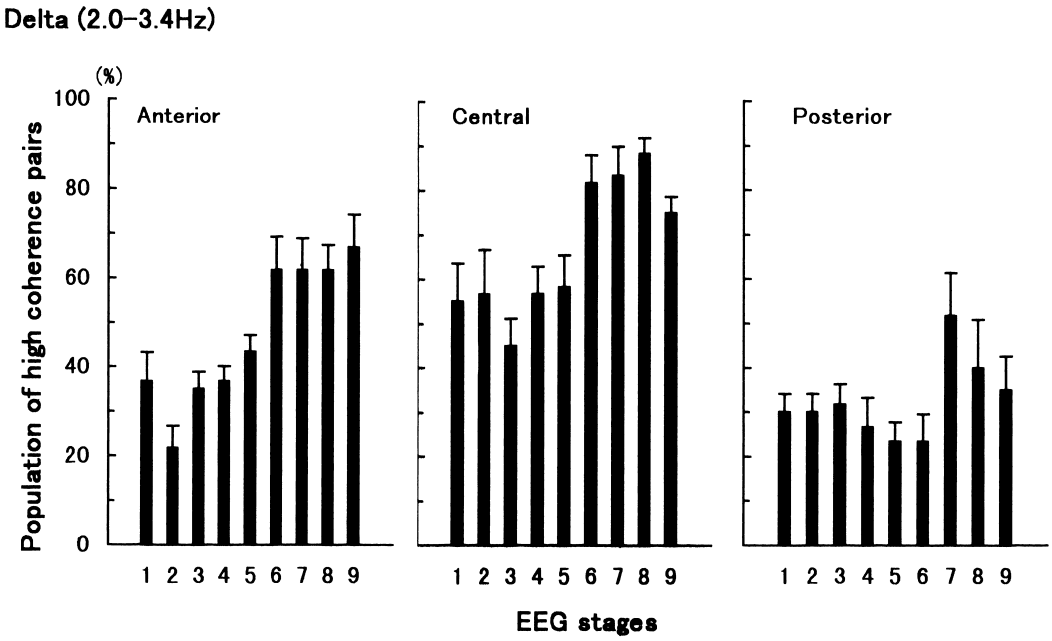

Fig. 7. Comparisons of percentages of high coherence pairs (coh ≥ 0.9: root coherence) in three equal areas of scalp for delta-band activity among nine EEG stages. The left panel shows the population of high coherence pairs for the anterior area. The central panel shows the population of high coherence pairs for the central area. The right panel shows the population of high coherence pairs for the posterior area. Vertical bars show the SEs. Anterior: Fp1, Fp2, F7, F8; central: Fz, C3, C4, Pz; posterior: T5,T6,O1,O2.

icantly. Regarding regional differences, significant region effects among anterior, central and posterior areas were obtained. The population of high coherence pairs (⩾0.9) in the anterior and central area were higher than that in the posterior area in EEG stages 4–9. Additionally, the population of high coherence pairs (⩾0.9) in the central area were higher than that in the anterior area in EEG stages 4–9. Eventually, the populations of high coherence pairs in the anterior and central areas begin to significantly increase not from EEG stage 5 (theta state), but from EEG stage 7 (vertex sharp wave bursts). These findings indicate that developments in inter- and intra-hemisphic coherence

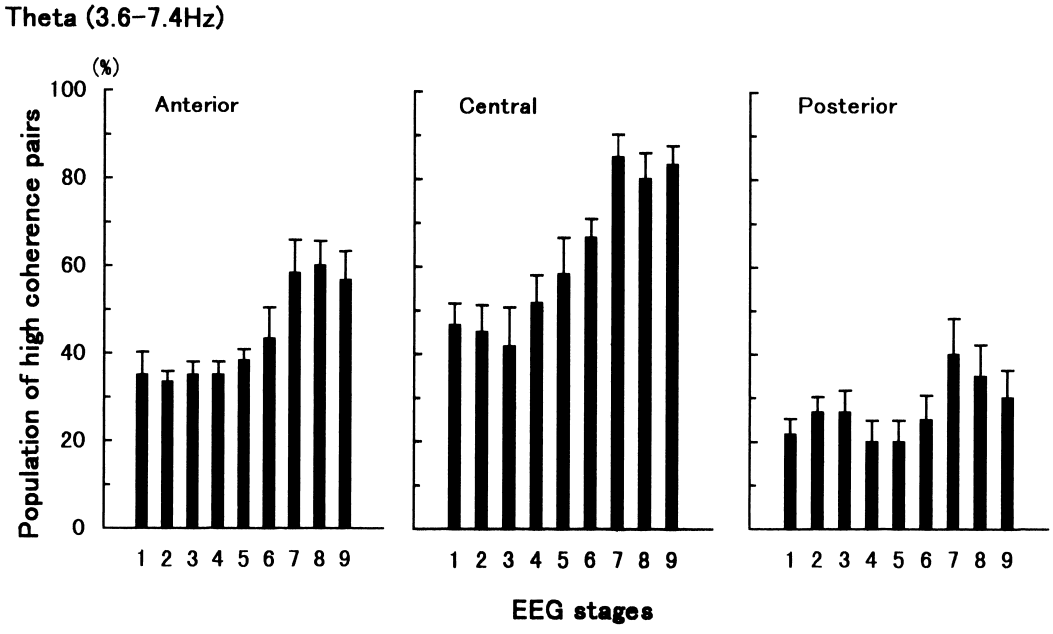

Fig. 8. Comparisons of percentages of high coherence pairs (coh ≥ 0.9: root coherence) in the 3 equal areas of scalp for theta-band activity among 9 EEG stages. See Fig. 7 for legend.

(synchronization) for theta-band activities are delayed in comparison to the appearance of theta waves. These results suggest that the dominant synchronous component of slow wave activities in the SOP increased as a function of EEG stages in the anterior-central areas and increased clearly after the appearance of vertex sharp waves.

4. Discussion

Topographic maps of coherence in delta- and theta-band activities demonstrated that the synchronous component at the anterior-central areas of the scalp appeared to correspond with increasing power. Furthermore, the present results suggested that slow wave activities in the anterior and central areas were more synchronized after the appearance of the vertex sharp wave. On the basis of these results, sleep onset process probably started before the onset of sleep stage 1 in standard criteria. On the other hand, the basic sleep process may start before the onset of the sleep stage 2 or the manually scored spindles. Ogilvie and Wilkinson (1984) introduced the concept of a sleep onset period (SOP), defined as the transition between relaxed, drowsy wakefulness and unresponsive sleep. So while the SOP may have sleep stage 1 at its center, it clearly overlaps into stage W and sleep stage 2 scored by standard criteria (Rechtschaffen and Kales, 1968). They examined changes in many measures (EOG, respiratory) based on behavioral responses to identify the point of sleep onset (Ogilvie and Wilkinson, 1984, 1988; Ogilvie et al., 1989). Additionally, Ogilvie et al. (1991) indicated that response cessation and abrupt increases in EEG power and amplitudes of ERP components converged to allow the researcher to identify the 'point' of sleep onset more clearly than ever before. Precisely when responses cease, EEG power increases across all frequencies, and these changes are accompanied by significant alternations in the nature of ERP; namely, sharp increases in P1, N2, N3 and P3 amplitude take place. They suggested that the electrical activity of the brain rapidly synchronizes during behavioral sleep onset. However, this study analyzed only the C_4 electrode and did not refer to spatial (topographical) aspects. In the present study, we examined the spatio-temporal behavior of synchronization in EEG activities, using coherence analysis. The present results showed that the population of high coherence pairs increased from EEG stage with vertex sharp waves in the anterior and central areas. Eventually, delta-band activity starts to synchronize rapidly in the anterior and central areas from the EEG stage with vertex sharp waves. In consideration that the appearance of the vertex sharp wave is related with behavioral sleep onset (Broughton, 1989; Hori et al., 1991, 1994), the results of the present study suggest that delta-band activities in the anterior and central areas rapidly synchronize and are accompanied with behavioral sleep onset. These results support those findings (Broughton, 1989; Hori et al., 1991, 1994) that the appearance of the vertex sharp wave is related to behavioral sleep onset.

Moreover, to compare the anterior area and the central area, the population of high coherence pairs ($\geqslant$0.9) in the anterior area maintained the same level after EEG stage 6, however, those of high coherence pairs ($\geqslant$0.9) in the central area peaked at EEG stage 8. These results indicate that the increase in the population of high coherence pairs is remarkable in the central area. Slow wave activity such as delta and probably extending to slow theta frequencies are considered to be of cortical origin and to reflect cortical inhibitory processes (Steriade et al., 1990). It is suggested that the increase of synchronous activities in the central area which is observed from the vertex sharp wave stage (EEG stage 6) may reflect the functional decrease of promoter cortex related to button pressing response. Furthermore, the populations of high coherence pairs of anterior area increased from EEG stage 6 (vertex sharp wave stage) and reached the level of EEG stage 9 earlier than those of other regions. In this context, the above findings supported these proposals (Wright et al., 1995; Tanaka et al., 1997) that sleep onset processes started in the anterior area including the premotor cortex then spread all over the scalp (i.e. sensory cortex). On the other hand, it is interesting that the population of high coherence pairs begin to increase not from EEG stage 5 (theta state), but from EEG stage 7 (vertex sharp wave bursts), significantly. These indicate that developments in inter- and intra-hemispheric coherence (synchronization) for theta-band activities were slightly delayed after the appearance of the theta wave. Hori et al. (1994) reported that the proportion of 'awake' response decreased below 50% after EEG stage 6 (vertex sharp wave stage). The functional decrease of frontal cortical region considered the seat of motivated attention (Tucker and Derryberry, 1992), reached the cortical level after EEG stage 6 (the vertex sharp wave stage) and caused attenuation of the feeling of being awake. However, the result of this study was obtained only by the alpha dominant normal young adult. It should be a bit more cautious in making general points regarding EEG coherence which are applicable to brain physiology. Therefore, in the near future, it would be necessary for comparative examinations to take, low alpha subjects, ages and sexuality into consideration.

Moreover, the influence of the use of the ipsilateral earlobe reference upon topographic variations in EEG activity should be considered, since amplitude of the EEG varies as a function of inter-electrode distance (i.e. the closer the electrodes, the smaller the potential difference). It is also important to consider the distance between the active EEG electrode and reference electrode sites. A reference electrode should be situated distant from many different sources. Although there is no perfect solution for these various reference electrodes position-related problems, recognition of the situation is important (Nuwer, 1988). In many conventional EEG studies, a contralateral or occasionally ipsilateral earlobe or mastoid reference is employed. Another

reference used especially in quantitative EEG studies involves linking electrodes placed on the earlobes. However, equalizing ear reference impedance is not easily done, and the effect of unequal impedance in a linked-reference configuration would be to artificially inflate the amplitude of the leads on the side of the reference electrode of highest resistance. In the present study, the dominant area of each band activity agreed with the findings of used ear-linked reference (Hasan and Broughton, 1994; Wright et al., 1995). The above findings may suggest that the contribution from the reference signal appears to require less consideration on understanding the topographical variation in this study.

Early investigators (Liberson and Liberson, 1966) maintained that slow eye movements (SEMs) were associated with drowsiness, and their reduction indicative of the entrance into sleep. Moreover, Rechtschaffen and Kales (1968) described slow eye movements (SEMs) as occurring early in the standard sleep stage 1. The possibility that SEMs have influence on the coherence in the frontal region should be considered. Therefore, speculation exists about this point. It is reported that SEMs were prominent in the standard sleep stage 1, which isn't accompanied by vertex sharp waves and that SEMs declined with deepening of sleep at the transition period of the standard sleep stage 2 (Hiroshige, 1987). The number of SEMs increases to a maximum during the process of falling asleep, but it begins to decrease before the standard sleep stage 2 (Hori, 1982). The SEMs tend to disappear with the appearance of sleep spindles, as arousal level becomes lower than that with SEMs (Liberson and Liberson, 1966). Thus, there appears to be an inverted U relationship between SEMs and sleep stages. Moreover, these reports suggest that the distribution of SEMs activities show an inverted U shape as a function of EEG stages. On the other hand, the coherence of slow wave activities started to increase as a function of EEG stages, and increased sharply in the anterior-central areas after the appearance of vertex sharp waves. These observations suggest that significant increases in the coherence values in the frontal region, which were not artifacts from horizontal SEMs. In other words, at the time when SEMs decrease, the increase of the coherence of slow wave activities are rather interesting.

The present results suggested that slow wave activities in the anterior and central areas were more synchronized after the appearance of the vertex sharp wave. Additionally, our results suggest that a detailed examination of the relationship between behavioral (reaction time: RT) and subjective (hypnagogic imagery: HI) measures on the 9 EEG stages during the transition from wakefulness to sleep will provide a cue for an all-inclusive study of the SOP. Moreover, further topographical analysis of alpha-band activities which were used as good indicators of waking level and sigma- band activities which correspond to sleep spindle activities might help distinguish the SOP from both wake and sleep and help clarify the psychophysiological structure of the SOP and its function. A better understanding of the variable phenomena of the SOP may lead to new insights into the links between brain function and behavior during waking and sleep states.

Acknowledgements

This study was supported by the Special Coordination Funds of the Japan Society for Promotion of Science.

References

Borbely AA, Baumann F, Brandeis D, Strauch I, Lehmann D. Sleep deprivation: effect on sleep stages and EEG power density in man. Electroenceph clin Neurophysiol 1981;51:483–493.

Broughton RJ. Evoked potentials and sleep-wake states in man. In: Horne J, editor. Sleep '88, Stuttgart: Gustav Fischer Verlag, 1989. pp. 6–10.

Davis H, Davis PA, Loomis AL, Harvey EN, Hobart G. Human brain potentials during the onset of sleep. J Neurophysiol 1938;1:24–38.

Dement WC, Kleitman N. Cyclic variation in EEG during sleep and their relation to eye movements, body motility and dreaming. Electroenceph clin Neurophysiol 1957;9:673–690.

Ford MR, Goethe JW, Dekker DK. EEG coherence and power in the discrimination of psychiatric disorders and medication effects. Biol Psychiat 1986;21:1175–1188.

Foulkes D, Vogel G. Mental activity at sleep onset. J Abnorm Psychol 1965;70:231–243.

Gibbs FA, Gibbs EL. Atlas of electroencepaphalography. Vol. 1, Cambridge: Addison-Wesley, 1950.

Guevara MA, Lorenzo I, Arce C, Ramos J, Corsi-Cabrera M. Inter- and intrahemispheric EEG correlation during sleep and wakefulness. Sleep 1995;18:257–265.

Hasan J, Broughton R. Quantitative topographic EEG mapping during drowsiness and sleep onset. In: Ogilvie RD, Harsh JR, editors. Sleep onset: normal and abnormal processes, Washington, DC: American Psychological Association, 1994. pp. 219–235.

Hiroshige Y. Variations of slow eye movements as an indicator of hypnagogic state. Jpn J Physiol Psychol Psychophysiology (in Japanese with English abstract) 1987;5:11–19.

Hori T. Electrodermal and electrooculographic activity in a hypnagogic state. Psychophysiology 1982;19:668–672.

Hori T, Hayashi M, Morikawa T. Topography and coherence analysis of the hypnagogic EEG. In: Horne J, editor. Sleep '90, Bochum: Pontenagel Press, 1990. pp. 10–12.

Hori T, Hayashi M, Kato K. Changes of EEG patterns and reaction time during hypnagogic state. Sleep Res 1991;20:20.

Hori T, Hayashi M, Morikawa T. Topographical EEG changes and the hypnagogic experience. In: Ogilvie RD, Harsh JR, editors. Sleep onset: normal and abnormal processes, Washington DC: American Psychological Association, 1994. pp. 237–253.

Liberson WT, Liberson CW. EEG records, reaction times, eye movements, respiration, and mental content during drowsiness. In: Wortis J, editor. Recent advances in biological psychiatry, New York: Plenum Press, 1966. pp. 295–302.

Murphy T, Ogilvie RD, Doerfing P, Alloway C, Lamarche C. Evaluation of Hori 9-stage sleep onset scoring system in unintentional sleep onset, narcolepsy and insomnia. Abst Jpn Soc Sleep Res 1999;24:137.

Nuwer MR. Quantitative EEG: Techniques and problems of frequency analysis and topographic EEG mapping. J Clin Neurophysiol 1988;5:1–43.

Ogilvie RD, Wilkinson RT. The detection of sleep onset: Behavioral and physiological convergence. Psychophysiology 1984;21:510–520.

Ogilvie RD, Wilkinson RT. Behavioral versus EEG-based monitoring of all-night sleep/wake patterns. Sleep 1988;11:139–155.

Ogilvie RD, Wilkinson RT, Allison S. The detection of sleep onset: behavioral, physiological, and subjective convergence. Sleep 1989;12:458–474.

Ogilvie RD, Simons IA, Kuderian RH, MacDonald T, Rustenburg J. Behavioral, event-related potential, and EEG/FFT changes at sleep onset. Psychophysiology 1991;28:54–64.

Rechtschaffen A, Kales A. A manual of standardized terminology, techniques and scoring system for sleep stages of human subjects, Washington DC: Public Health Service, US Government Printing Office, 1968.

Shaw JC. Correlation and coherence analysis of the EEG: a tutorial review. Int J Psychophyol 1984;1:255–266.

Shiotsuki M, Ichino Y, Shimizu K. Changes in the electroencephalogram during whole night natural sleep. Jpn J Surg Soc 1954;55:322–331.

Steriade M, Gloor P, Linas RR, Lopes de Silva FH, Meaulam MM. Basic mechanisms of cerebral rhythmic activities. Electroenceph clin Neurophysiol 1990;76:481–508.

Tanaka H, Hayashi M, Hori T. Statistical features of hypnagogic EEG measured by a new scoring system. Sleep 1996;19:731–738.

Tanaka H, Hayashi M, Hori T. Topographical characteristics and principal component structure of the hypnagogic EEG. Sleep 1997;20:523–534.

Tanaka H, Hayashi M, Hori T. The Dominant topographic component of hypnagogic EEG. Psychiat Clin Neurosci 1995;49:44.

Tucker DM, Derryberry D. Motivated attention: Anxiety and the frontal executive functions. Neuropsychiat Neuropsychol Behav Neurol 1992;5:233–252.

Winer BJ, Brown DR, Michels KM. Statistical principles in experimental design, third ed. New York: McGraw-Hill, 1991.

Wright Jr KP, Badia P, Wauquier A. Toporaphical and temporal patterns of brain activity during the transition from wakefulness to sleep. Sleep 1995;18:880–889.